Hindawi
Mobile Information Systems
Volume 2022, Article ID 1534596, 12 pages
https://doi.org/10.1155/2022/1534596

Research Article

Automatic Recognition and Repair System of Mural Image Cracks Based on Cloud Edge Computing and Digitization

Yongli Gao[1] **and Zijie Zhou**[2]

[1]*National Experimental Teaching Demonstration Center of Design Art, Taiyuan University of Technology, Taiyuan 030024, Shanxi, China*
[2]*College of Art, Taiyuan University of Technology, Taiyuan 030024, China*

Correspondence should be addressed to Yongli Gao; gaoyongli@tyut.edu.cn

Received 2 August 2022; Revised 1 September 2022; Accepted 27 September 2022; Published 10 October 2022

Academic Editor: Muhammad Zakarya

Mural painting is the art on the wall, it is the painting that people draw on the wall, it is one of the earliest forms of painting in human history, and it is also an accessory part of the building. The decorative and beautifying functions of murals make them an important aspect of environmental art. Cloud edge computing is a combination of cloud computing and edge computing, that fully absorbs the advantages of both cloud computing and edge computing and maximizes their advantages. In this study, based on cloud edge computing and digital technology, the automatic identification and repair system of fresco image cracks is studied. Image segmentation techniques have been proposed in this study, using 60 murals in three regions as experimental objects. Through experimental analysis, it is found that the traditional pine poise treatment method takes the shortest repair time. However, for a specific image, it is difficult to guarantee the quality of its restoration. The mural image in area A was repaired with the conventional pine pitch repair method, which took 113.01 seconds, and the subjective evaluation was 69 points. Using the repair method described in this study to repair, it takes 127.38 seconds, and its subjective evaluation score is the highest, which is 87 points. The experimental results have shown that the cloud edge computing method and digital technology have had a certain positive effect on the identification and repair system of fresco image cracks.

1. Introduction

As one of the types of cultural relics, frescoes represent the production and living conditions of the society at that time in the form of pictures by the ancients and are an important basis for scholars to study ancient civilizations. Due to factors such as geological activities and human damage, the painted murals have been damaged in various forms such as cracks, fading, and oxidation, and these damaged murals continue to be repaired, but traditional handicraft techniques find it difficult to complete such difficult task. Using computer technology to digitally repair damaged murals, on the one hand, the damaged murals can be repaired in time, and on the other hand, it is also helpful for the virtual display of the murals. For the problem of damaged murals, traditional manual techniques were used to restore them in the past. However, due to the lack of talent, it is difficult to restore a large number of cultural relics in a short period of time. Therefore, the innovation of this study is to use the cloud edge computing method and digital technology to perform image processing on the fresco crack image, automatically identify the crack type, and perform image repair.

The advent of the digital age has greatly facilitated work and life. This study has carried out a comprehensive study of cloud edge computing methods, digital technology, and mural crack identification and repair systems. The innovation of this study is using image processing technology,

noise processing of mural images, and research on image threshold segmentation. Therefore, the role of cloud edge computing methods and digital technology in fresco crack identification research is effective. To a certain extent, it can save manpower and material resources and speed up the restoration of murals.

2. Related Work

With the expansion of human activities, various murals have been discovered. Affected by various natural factors and human activities, the frescoes have problems such as cracks and damages, which need to be identified and repaired using technology. Many scholars have conducted research on this. Wang has proposed using the needs of users in daily life to discuss ways to expand image access points. Due to the advanced Internet and digital technology, as well as the characteristics of the younger generation, images have been searched and used extensively [1]. Patayon and Crisostomo have proposed to develop an automatic identification system for abaca bunchy top disease using different deep learning models [2]. Conforto et al. have proposed a robot-assisted treatment method and have used an automatic identification system to identify the patient's disease type, which has assisted doctors to make better treatment plans [3]. Mu and Yue have proposed to classify and grade the image degradation of security signs, trying to break the limitation of real-time image recognition [4]. Chen et al. have proposed the establishment of a comprehensive prediction model, which has integrated the medical imaging features of patients and has purposefully identified and classified the disease types of patients [5]. The above studies have applied automatic recognition and repair systems to various fields of research, but few have used automatic recognition systems for crack recognition in mural images.

In recent years, cloud edge computing methods have continued to develop, and digital technologies have also been popularized. Scholars from all walks of life have used cloud edge computing methods and digital technologies to conduct research on various academic issues. Chen and Wang have argued that nonintrusive load monitoring can infer the operating status of equipment and its energy consumption by analyzing energy data collected from monitoring equipment. With the rapid increase in the number and types of electrical loads, the traditional way of uploading all energy data to the cloud faces huge challenges [6]. Xu et al. have believed that cloud edge computing already has powerful real-time information collection capabilities and has played a vital role in providing diversified services. It works by transferring the collected information to a centralized, resource-intensive cloud platform for service implementation [7]. Taleb et al. have considered multiaccess edge computing as a platform designed to converge telecom and IT services to provide cloud computing at the edge of the radio access network [8]. Ogino et al. have proposed a flexible multiagent-based IoT edge computing architecture for balancing cloud global and edge local optimization and optimizing the roles of cloud servers and edge servers [9]. Esposito et al. have considered that one of the advantages of connecting edge computing and cloud computing is to achieve high throughput with real-time processing to ensure data durability [10]. The above research is a good analysis and application of cloud edge computing, but the field of application rarely involves the identification of cracks in mural images.

3. Recognition and Repair Method for Cracks in Mural Images under Cloud Edge Computing and Digitization

3.1. Crack Identification and Repair of Mural Images. Murals are the precious historical and cultural heritage of human beings and an important means of reflecting ancient civilizations and have high artistic value. Due to their existence, the ancient murals have various problems with cracks and damage, and it is necessary to use the current technology to repair the murals [11]. As shown in Figure 1, it is an image of an ancient mural.

The problems with murals are mainly cracks, falling off, fading, and herpes [12, 13]. With the passage of time, the damage from the strokes will be more serious, so the protection of the murals is imminent. As shown in Figure 2, it is a common problem in murals.

According to relevant information, most of the ancient murals appeared in ancient temples, as shown in Figure 3.

It can be seen from Figure 3 that the above images are murals taken at Jueshan Temple, Kaihua Temple, Sansheng Temple, and Yanshan Temple, respectively.

3.2. Cloud Edge Computing Methods and Digital Technologies. The digitization of cultural relics integrates modern information technology for the protection of cultural relics, and as a new development trend, the digitization of cultural relics is also used by cultural relics protection units around the world [14]. Based on the cloud edge computing method and digital technology, this study uses image preprocessing technology to study the problem of fresco cracks [15]. As shown in Figure 4, it is an introduction diagram for the image preprocessing system.

Image processing is to process the information collected by the image acquisition system. Due to the influence of various factors, the collected information may have certain problems [16, 17]. Moreover, because of the huge number of crack images in murals, in order to extract information quickly, it is necessary to denoise the images first.

Noise introduction: in the process of generation, transmission, and storage, images are prone to noise [18]. This study selects the most common Gaussian noise and salt and pepper noise for analysis.

3.2.1. Gaussian Noise. If Gaussian noise is regarded as a variable in the image, the probability density function formula of noise is as follows [19]. Gaussian function means

Figure 1: Ancient mural image.

Figure 2: Frequently asked questions about murals.

that the probability density function of the modified noise obeys a normal distribution:

$$Q(m) = \frac{1}{\sqrt{2\pi}\alpha} e^{-(m-\nu)^2/(2\alpha^2)}, \tag{1}$$

where m is a variable, ν represents the expected value of m, α represents the standard deviation of m, and α^2 represents the variance of m.

3.2.2. Salt and Pepper Noise. This noise is caused by the photoelectric conversion process of image sensors and other devices and appears as irregular and dark dots in grayscale images [20]. If salt and pepper noise is used as a variable, the probability density function formula for noise is as follows:

$$Q(m) = \begin{cases} Q_a & m = a \\ Q_b & m = b \\ 0 & \text{others} \end{cases}, \tag{2}$$

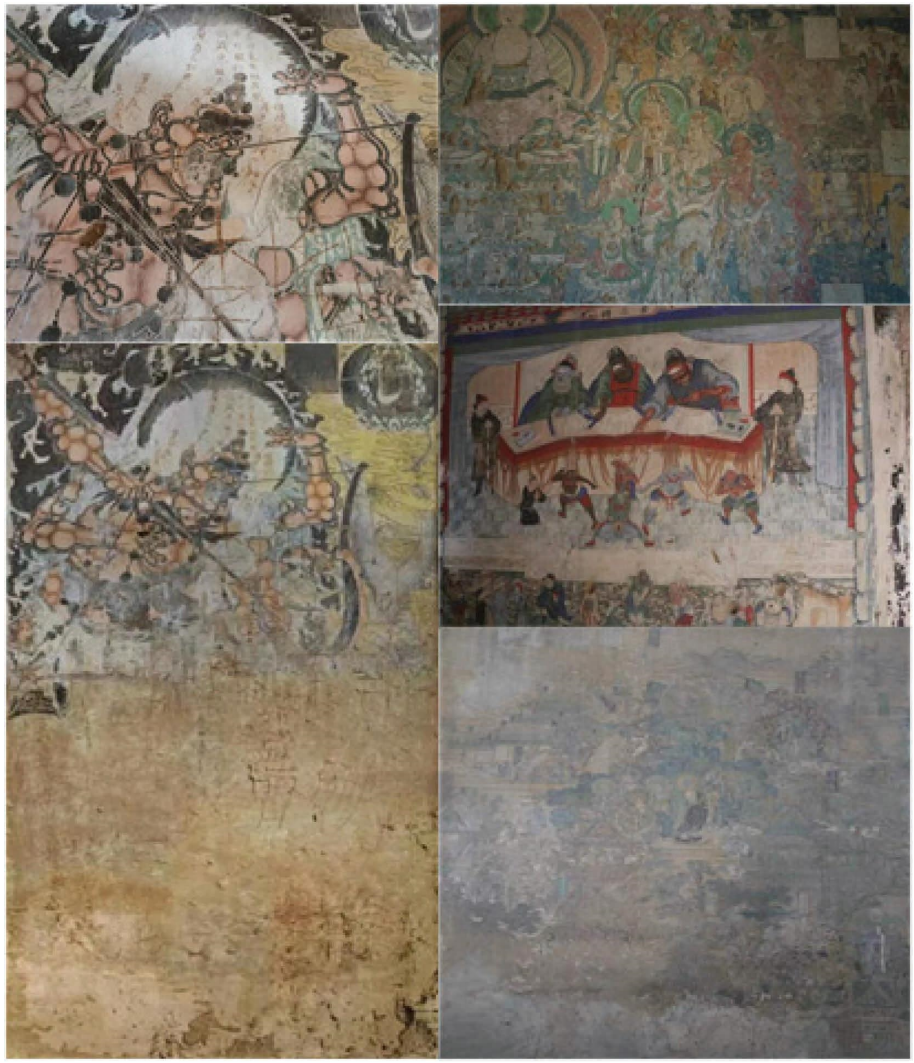

Figure 3: Ancient murals in the temple.

where $0 \le Q_a \le 1$ and $0 \le Q_b \le 1$. Usually, the pulse value of salt and pepper noise is divided into positive and negative numbers, and the pulse intensity is much larger than that of the image signal, so an image is always numerically converted to the maximum value, that is, pure black or pure white. For noise processing, denoising is required. There are many denoising methods. This study mainly introduces three denoising methods: mean filter, median filter, and Wiener filter [21]. It is as follows.

3.2.3. Mean Filtering. It is because the original pixel in the image and the surrounding pixels are related, but the noise does not have this correlation [22]. Therefore, this property can be used to replace the gray value of the target pixel with the gray value of the pixel in the field, thereby achieving the purpose of reducing sharp noise [23]. As shown in Figure 5, it is a graph of the mean filter model.

The formula is as follows:

$$f(m,n) = \frac{1}{X} \sum_{x,y \in R} g(m,n), \tag{3}$$

where $g(m,n)$ represents the gray value of the original image pixel, $f(m,n)$ represents the gray value of the processed image pixel, and $x * y$ represents the field window size.

3.2.4. Median Filtering. It sorts all the pixels in the field according to the gray value and takes the gray median value to replace the gray value of the target pixel [24]. The characteristics of this method are similar to those of the mean filter; that is, the substitute index is replaced by the median value. This method is simple and convenient to calculate, but the phenomenon of image blurring will also occur. The specific formula is as follows:

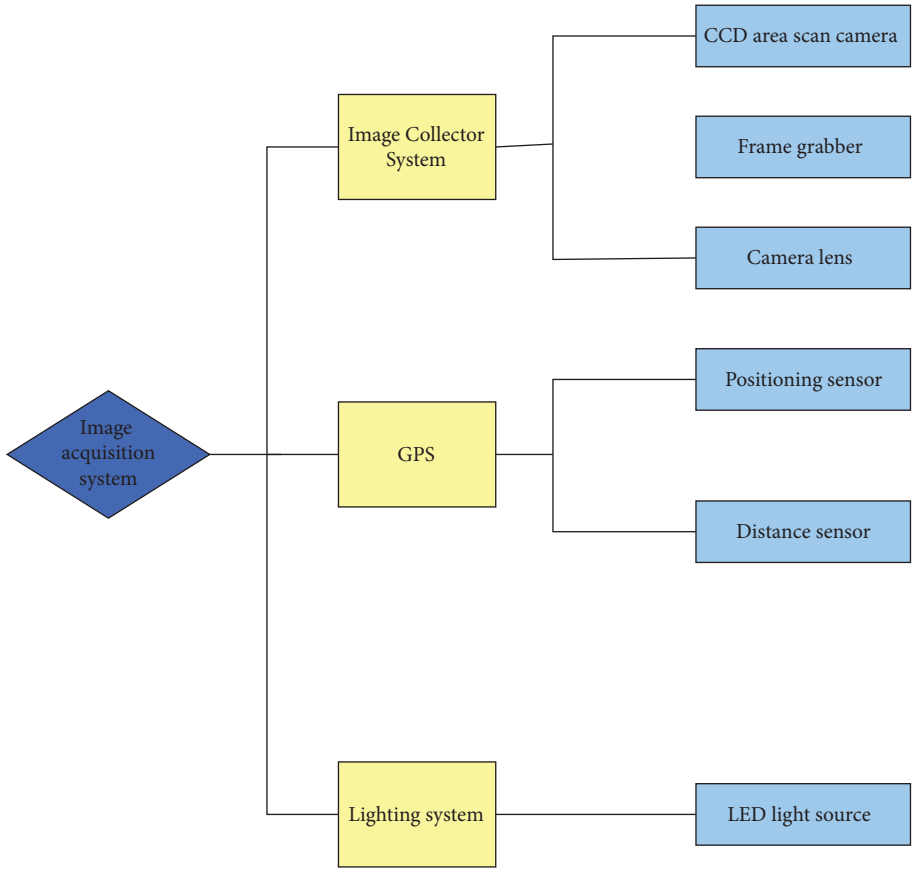

Figure 4: Introduction to the image preprocessing system.

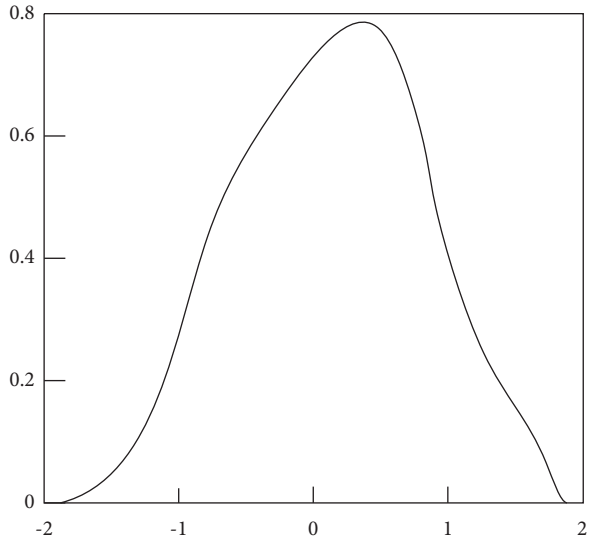

Figure 5: Mean filter model diagram.

$$f(m,n) = \mathrm{med}\{g(m_1,n_1), g(m_X,n_X)\}, \quad (4)$$

where $g(m,n)$ represents the gray value of the original pixel, $f(m,n)$ represents the gray value of the processed image pixel, and X represents the number of pixels in the field.

3.2.5. Wiener Filtering. Wiener filtering is an optimal filtering method using the minimum mean square error criterion under stationary conditions. Its central idea is to find an optimal linear filter that minimizes the value of the mean square error [25]. As shown in Figure 6, it is a diagram of the Wiener filter model.

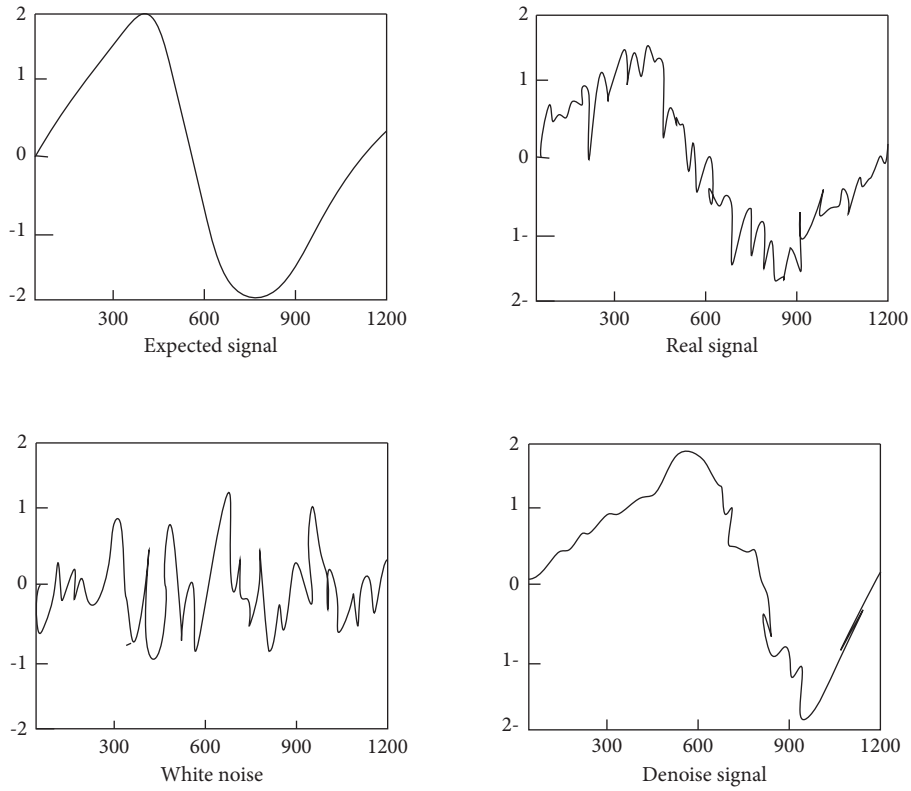

Figure 6: Wiener filter model diagram.

Its formula is as follows:

$$\nu = \frac{1}{X \times Y} \sum_{m,n \in R} g(m,n),$$

$$\alpha^2 = \frac{1}{X \times Y} \sum_{m,n \in R} (g(m,n) - \nu)^2, \tag{5}$$

$$f(m,n) = \nu + \frac{\alpha^2 - z^2}{\alpha^2} (g(m,n) - \nu),$$

where g (m, n) represents the original image pixel gray value, f (m, n) represents the processed image pixel gray value, v represents the average gray value of the pixel in the field, α^2 represents the grayscale variance of pixels in the field, and α^2 represents the overall grayscale variance of the image. According to the formula of Wiener filtering, it can be seen that this method can change with the local variance of the image. When the local variance increases, a weaker smoothing process will be performed. Stronger smoothing is performed when the local variance is reduced [26]. For crack images, the smaller the gray variance of the background, the larger the gray variance of the edge region of the crack, so Wiener filtering can fully preserve edge information under a smooth background.

Image threshold segmentation research: a binary image refers to an image with only two gray levels of 0 and 1, that is, a black and white image. The process of converting a multigray level image into a binary image is called image segmentation. Image segmentation has two methods: edge detection and region similarity.

In segmentation based on regional similarity, threshold segmentation has been widely used in practice due to its simple operation and strong practicability. Threshold segmentation mainly selects a threshold and uses the threshold to segment the image. The formula is as follows:

$$f(m,n) = \begin{cases} 0, & g(m,n) < T \\ 1, & g(m,n) \geq T \end{cases}, \tag{6}$$

where $g(m,n)$ represents the pixel gray value of the original image, $f(m,n)$ represents the processed image gray value, and T represents the threshold. It can be seen from the formula that when the gray value of the pixel in the image is lower than the set threshold, the gray value will be redefined as 0. That becomes the black point. When the gray value of the pixel point of the image is higher than the set threshold, the gray value is redefined as 1, that is, the white point. As shown in Figure 7, images with different thresholds are segmented.

A threshold is selected to segment all pixels of the entire image. Under the dynamic threshold, different thresholds should be selected at different positions for segmentation. The following is an introduction to several commonly used image algorithms.

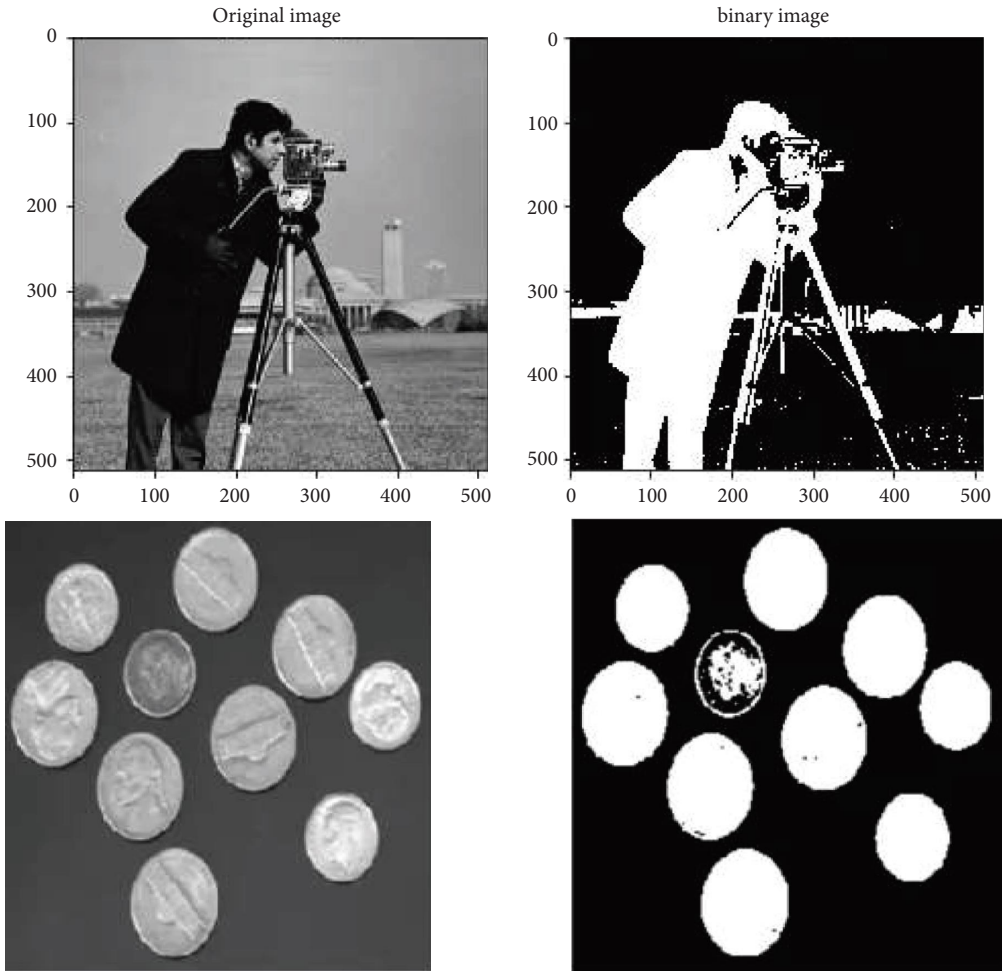

Figure 7: Segmentation of images with different thresholds.

(1) Maximum Entropy Method. Entropy indicates that an information source is uncertain and reflects the amount of information in the image. When the amount of information in the image is larger, the entropy of the image will also increase.

Suppose that an image size is $X \times Y$, the gray level is 0~K, the number of pixels with gray level i in the image is Y_i, and the ratio of each gray level in the image is

$$Q_i = \frac{Y_i}{X \times Y}, i = 0, 1, 2, K, \quad \sum_{i=0}^{K} Q_i = 1, \tag{7}$$

where Q_i represents the probability that each gray level accounts for the entire image.

Set the initial threshold T, and divide the image into two parts a, b, where a represents the image of the target area and b is the image of the background area; then,

$$\begin{aligned} H_a(T) &= -\sum_{i=1}^{T} \frac{Q_i}{Q_a} \log \frac{Q_i}{Q_a}, \\ H_b(T) &= -\sum_{i=1}^{T} \frac{Q_i}{Q_b} \log \frac{Q_i}{Q_b} = -\sum_{i=1+T}^{T} \frac{Q_i}{1-Q_a} \log \frac{Q_i}{1-Q_a}, \\ Q_a &= \sum_{i=0}^{T} Q_i, Q_b \\ H(T) &= H_a(T) + H_b(T), \\ H(T') &= \max H(T), \end{aligned} \tag{8}$$

where $H_a(T)$ represents the entropy of area a, $H_b(T)$ represents the entropy of area b, $H(T)$ is the sum of the entropy of area a and area b, and T' represents the optimal threshold.

(2) Maximum Interclass Method. The maximum interclass method refers to considering the image as two parts, namely, the background and the target, using variance to represent the difference between the background and the target, and

finding an optimal threshold to maximize the interclass variance in this part.

Assuming that the size of the image is $X \times Y$, the gray level is 0~K, and the number of pixels whose gray level is i in the image is N_i; then, the probability that each gray level occupies the entire image is

$$Q_i = \frac{N_i}{X \times Y}, i = 0, 1, 2, K, \quad \sum_{i=0}^{K} Q_i = 1. \tag{9}$$

Set the initial threshold and divide the image into two parts, a and b; then,

$$Q_a = \sum_{i=0}^{T} Q_i, Q_b = \sum_{i=T+1}^{T} Q_i, \quad \nu_0 = \sum_{i=0}^{T} iQ_i, \nu_a = \sum_{i=0}^{T} i\frac{Q_i}{Q_a}, \nu_b = \sum_{i=T+1}^{T} i\frac{Q_i}{Q_b}, \tag{10}$$

where Q_a represents the probability that the pixels in the area a occupy the entire image, Q_b represents the probability that the pixels in the area b occupy the entire image, ν_0 is the grayscale mean of the entire image, ν_0 is the grayscale mean of the area a, and ν_0 is the grayscale mean of the area b.

The formula for the between-class variance α^2 is

$$\alpha^2 = Q_a(\nu_a - \nu_0)^2 + Q_b(\nu_b - \nu_0)^2. \tag{11}$$

The maximum interclass method is to select the best threshold, T', to maximize the interclass variance, and its formula is

$$\alpha^2(T') == \max \alpha^2(T). \tag{12}$$

The maximum between-class method is usually used in the case where the target and the background of the image are quite different.

In the case where the variance value of the target and the background is not much different, the maximum between-class method makes it difficult to obtain a better segmentation method.

4. Experimental on Crack Identification and Repair in Mural Images

4.1. Experimental Results of Crack Identification and Repair in Mural Images. For the automatic identification and repair system of fresco image cracks, this study mainly conducts a statistical analysis of the problems of ancient frescoes. Twenty murals in three regions of A, B, and C were selected as the research objects. Due to the differences in natural conditions such as climate, the murals in the three regions were damaged differently. Details are as follows.

4.1.1. Problems with Murals. Due to the influence of natural factors, the frescoes in the three regions have different degrees of problems, the most important of which are cracks, fading, and damage. The specific situation is shown in Figure 8.

As can be seen from Figure 8, among the 20 murals in area A, 19 murals have cracks, 10 murals have faded, and 4 murals have broken and missing pieces. In area B, 3 frescoes have cracks, 7 frescoes have fading problems, and 13 frescoes are found to be missing pieces. In Area C, 15 murals have cracks, 13 have faded, and 18 have missing blocks. From these data, it can be seen that some of the murals in the three regions may have more problems, such as cracks, missing pieces, and fading problems.

It can be found from the figure that the murals in areas A and B have fewer problems than the murals in area C. However, due to the difference in climatic factors between A and B, the problems of murals in the two places take on opposite forms. Among them, area A has a high temperature and a dry climate all year round, so the air humidity is low, and the walls of the murals are dry and easy to crack, so the murals have more cracks and fading. Area B is rainy all year round, and the climate is humid. The walls of the murals are wet, so the walls are easy to peel off, and there are cases of missing pieces and damage. However, due to the extreme climatic conditions in the C area, the dry season and the rainy season are distinct, the dry season is hot and dry, and the rainy season is also hot and rainy, which leads to more problems with the murals in the C area. The problems of cracks, missing blocks, and fading are more serious than those in the other two areas. This shows that climatic factors will affect the state of the murals.

4.1.2. The Time When the Murals Existed. Due to the existence of ancient murals for too long, it will also cause problems such as damage to the murals. The specific situation is shown in Figure 9.

It can be seen from Figure 9 that most of the murals in area A have a history of over 1000 years, and some murals are less than 1,000 years old. Among them, there is one under 500 years old, accounting for only 5%. There are 2 pictures from 500 to 1000, accounting for 10%. There are 17 murals over 1000 years old, accounting for as high as 85%; it also reflects from the side that region A has a long history and human activities occurred earlier. Most of the frescoes in area B are more than a thousand years old. Among them, there are 2 murals under 500 years old, accounting for 10%. There are 3 murals from 500 to 1000, accounting for 15%. There are 15 murals over a thousand years old, accounting for 75%. This also shows that the historical civilization of the B region is relatively long. Among the murals in area B, there is 1 mural with horizontal cracks, 3 with vertical cracks, 2 with shedding, and 2 with massive cracks. Compared with the mural history of the other two regions, the history of the murals in the C area is relatively short. Among them, there are no murals under 500 years old, 18 murals are 500 to 1000 years old, accounting for 60%, and 2 murals are more than 1000 years old, accounting for 20%. This shows that the

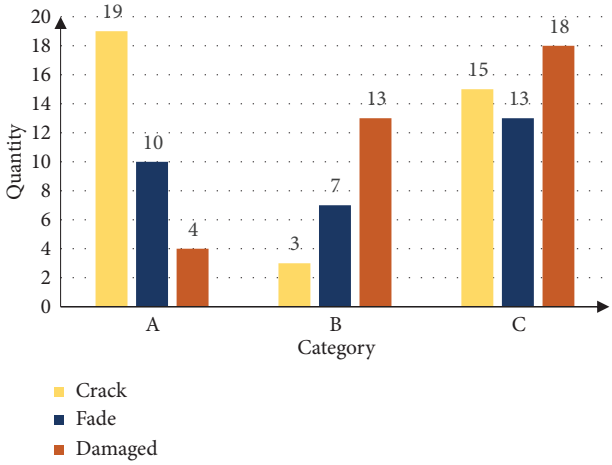

Figure 8: Problems with murals in three regions.

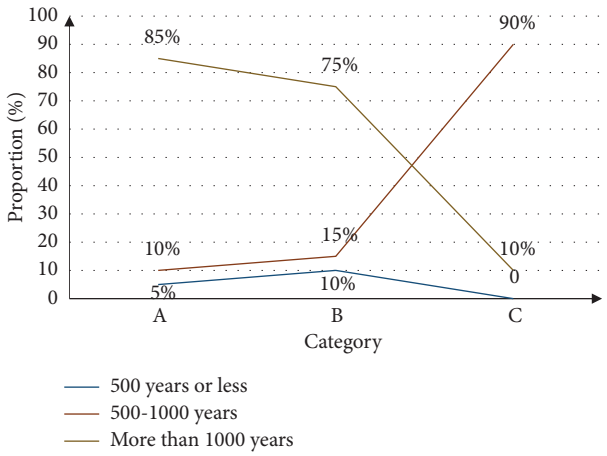

Figure 9: How long did the frescoes exist?.

frescoes in the C area mainly appeared 500 years ago, when there were frequent human activities in the area. It can be seen that the appearance time of the murals can also understand the time when the local historical civilization appeared. Due to the existence of murals for too long, it will also lead to various problems with murals.

4.1.3. The Form of Cracks in the Frescoes. This paper mainly studies the identification and repair system of fresco cracks. This study conducts experiments on different cracks since the appearance of cracks is usually accompanied by problems such as wall peeling and water seepage. The specific crack form is shown in Figure 10.

It can be seen from Figure 10 that there are cracks in the murals in the three areas. Among them, there are many cracks in the murals of A and C. There are 19 murals with horizontal cracks in the murals in Area A. There are 12 frescoes with longitudinal cracks. There are 9 cases of falling off. There are 15 frescoes with blocky cracks. Among the murals in Area C, there are 13 murals with horizontal cracks, 14 with longitudinal cracks, 11 with falling off, and 15 with

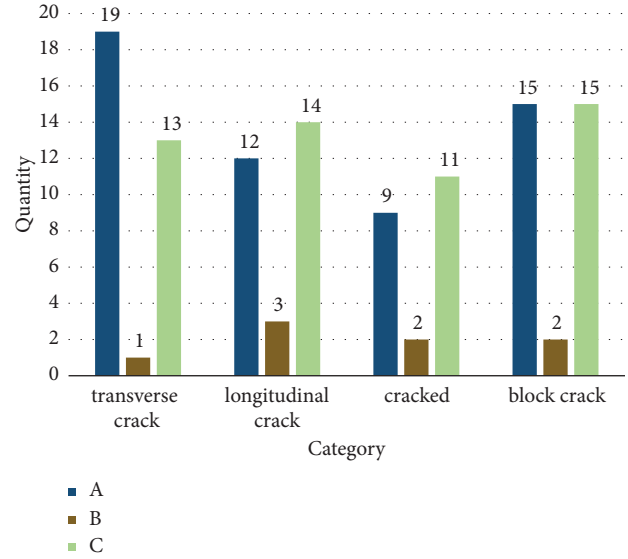

Figure 10: The fresco appears in the form of cracks.

massive cracks. Cracks in different directions and shapes are due to local geological activities, human activities, climate, and other factors that cause different degrees of cracks in the murals.

In order to facilitate comparison, a representative mural was selected from each of the three regions for comparative analysis, and the restoration time and various restoration indicators of the crack image of the mural are listed in a table, as shown in Table 1.

It can be seen from Table 1 that the number of repaired pixels in the repaired image is directly related to the repair time. The more pixels to be repaired, the longer the repair time. The number of repaired pixels can reflect that the search range of the sample block affects the repairing time, and the ratio of repaired pixels to total pixels can also reflect the difficulty of image repairing. The frequency of replication of the samples can reflect the complexity of the cracks in the frescoes to be repaired. The ratio of Poisson processing times to sample replication times is an important comparison parameter. It can be seen from Table 1 that the restoration time of the three murals is calculated in seconds, which is an acceptable restoration time length. The proportion of repaired pixels to total pixels is 3.6%, 7.7%, and 21%, respectively. Different proportions indicate that the difficulty of repairing will also be different. The repairing is achieved for three sets of images to be repaired with different proportions, which shows the effectiveness of the repairing method in this study. In the three groups of experiments, the number of Poisson processing accounted for about 25% of the total number of sample replications, which indicates that the Poisson processed method repaired only the initial outermost sample block as expected. In the field of image restoration, there is still no clear definition of the restoration effect. In the past restoration process, the peak signal-to-noise ratio is often used. Because the object removal experiment does not have known images as a comparison benchmark, which makes the metric difficult to calculate

Table 1: The repair metrics of the algorithm in this study.

	A	B	C
Repair time (s)	131.39	198.62	98.29
Fix pixel (per)	3568	6629	12656
Total pixels (per)	97415	97314	61438
Sample replication times (times)	125	211	221
Number of Poisson treatments (times)	22	47	38

accurately, this kind of experiment cannot be applied to the inpainting experiment. This experiment uses a subjective evaluation strategy; that is, the experimenter evaluates the repaired images without knowing the repaired area.

It can be seen from Table 2 that this experiment has achieved relatively good results in terms of restoration time and restoration quality. The traditional loose poise processing method takes the shortest restoration time, but for a specific image, it is difficult to guarantee the restoration quality. As can be seen from Table 2, the frescoes in area A were repaired by the conventional pine poise repair method, which took 113.01 seconds and the subjective evaluation was 69 points, while the restoration using the Criminisi repair method took 139.45 seconds and the subjective evaluation was 83 points. Using the repair method in this study to repair, it only takes 127.38 seconds and its subjective evaluation score is the highest, which is 87 points. Although the repair method in this study takes a long time, it can guarantee the quality of its repair. The mural image in area B was repaired with the conventional pine poise repair method, which took 186.66 seconds and the subjective evaluation score was 65 points, while the restoration using the Criminisi repair method took 221.06 seconds and the subjective evaluation score was 69 points. The repair method in this study was used. To repair, it takes 193.12 seconds to use, and the subjective evaluation score is as high as 83 points. To sum up, the repair method described in this study has obvious advantages in repair effect compared with other repair methods, and its evaluation score and repair quality are both high.

It can be seen from Table 3 that image inpainting can be used for image compression, but since the inpainting principle of image inpainting technology is to use the correlation of the image itself, the prerequisite for applying image inpainting technology to image compression is that the image content has a certain correlation. If the correlation of the image is large, a larger compression ratio can be obtained, but if the image itself is an image with less correlation and more complex cracks, the compression ratio will be reduced accordingly. For example, the fresco images in area C have more complex cracks, and the compression ratio will be lower than the compression ratio of the murals in areas A and B. Among the compression ratios of the mural images in the three regions, the highest compression ratio is the mural image in Region A, whose ratio is less than 5 : 1. The compression ratios obtained in the mural images in the three regions are the maximum values obtained under the premise that the restoration algorithm studied in this paper can be restored, and the existing restoration algorithms have made it difficult to complete the restoration task. Theoretically speaking, with the development of image inpainting technology, a higher compression ratio can be obtained under the condition that the new inpainting technology has more powerful inpainting capabilities.

4.2. Improve the Experimental Scheme of Crack Identification and Repair in Mural Images. According to the above analysis, the cloud edge computing method and digital technology are perfectly combined with the research on the fresco crack identification and repair system. The idea of identifying, analyzing, and repairing cracks in frescoes with digital technology has greatly facilitated scholars' research on this project. However, because the learning on digital technology and cloud edge algorithms is not deep and complete enough, the experiments in this study still have some defects, which need to be improved. The details are as follows. First, in the three regions of A, B, and C as the experimental objects, the selected sample size is not enough, and the number of samples needs to be increased to ensure the accuracy of the experimental results. Second, in the experiment, only the Criminisi repair method and the loose Pois repair method were selected as the comparison methods. It is recommended to add several types of repair algorithms, and the results obtained will be different, and the reliability will also increase. Criminisi repair method is difficult to ensure the repair quality of the edge with a strong structure, and the phenomenon of structural disconnection may occur. The loose Pois repair method also has certain defects. Since the size of the sample block is fixed, the repair process is not flexible enough, and error repair may occur.

5. Discussion

With the development of Internet technology, it has become the daily work of experts and technicians to use computer technology to restore the treasures of cultural relics that were difficult to restore manually in the past. In this study, the identification and repair system of fresco cracks has been studied by combining cloud edge computing methods with digital technology. There are still several problems in the research process of this study. (1) The repair algorithm in this study is not perfect, the repair time is too high, and the subjective evaluation score is too low. (2) For more complex cracks, the repair technology in this study is difficult to completely repair and it is difficult to completely repair them. (3) The experimental subjects selected in this study are too few, the number of comparable samples is small, and the reliability of the experimental results is not high. In this regard, there is still a long way to go to completely repair the cracks in the murals using computer technology.

This study is devoted to the research based on cloud edge computing methods and digital technology in various fields and applied to the analysis of mural crack repair technology. A new attempt has been made in the study of fresco crack identification and repair systems. Through the case study, it is shown that this study reflects the effectiveness of the cloud edge computing method and digital technology in the analysis of the mural crack repair system.

Table 2: Comparison of repair evaluation and repair time.

		Regular Poisson processing fix	Criminisi repair	How to fix this article
A	Subjective evaluation (score/total score)	69/100	83/100	87/100
	Repair time (s)	113.01	139.45	127.38
B	Subjective evaluation (number of approvals/samples)	65/100	69/100	83/100
	Repair time (s)	186.66	221.06	193.12
C	Subjective evaluation (score/total score)	54/100	77/100	89/100
	Repair time (s)	91.24	111.43	98.21

Table 3: Comparison of compression repair schemes.

	Original size (KB)	Size after compression (KB)	Compression ratio (%)	AIEI model PSNR (dB)	CDD model PSNR (dB)	The method of this paper PSNR (dB)
A	67	16	21.09	26.3	25.4	27.3
B	67	15.8	21.88	31.3	28.7	35.2
C	87	27.3	33.73	31.6	27.9	32.3

6. Conclusions

This study has taken digital technology as the main analysis technology and has taken 20 murals in three regions A, B, and C as the research objects. Statistical analysis has been carried out on the problems of each mural, and the cloud edge computing method and digital technology have been used to classify them and identify the shape of the cracks in the mural. Through the case study, it has been concluded that factors such as temperature, humidity, precipitation, geological activity, and time can cause various problems such as cracks and fading of murals. The higher the image compression technology and the higher the image compression ratio, the higher the completeness of image restoration. The length of image restoration time does not guarantee the quality of image restoration. To sum up, the research on the fresco crack identification and repair system needs more in-depth and systematic analysis. The research in this study is only based on image pixels, recognition time, and image compression technology. The research of fresco crack repair based on cloud edge computing methods and digital technology has been a popular research object among experts and scholars from all walks of life in recent years, and further research is needed at present.

Data Availability

Data sharing not applicable to this article as no datasets were generated or analyzed during the current study.

Conflicts of Interest

The authors declare that they have no conflicts of interest with any financial organizations regarding the material reported in this study.

Acknowledgments

This work was the research result of the 2021 Shanxi Provincial Art and Science Planning Project "Research on the digital dynamic translation and communication path of Shanxi temple murals" (no. 2021c020).

References

[1] X. Wang, N. Song, L. Zhang, and Y. Jiang, "Understanding subjects contained in Dunhuang mural images for deep semantic annotation," *Journal of Documentation*, vol. 74, no. 2, pp. 333–353, 2017.

[2] U. B. Patayon and R. V. Crisostomo, "Automatic identification of abaca bunchy top disease using deep learning models," *Procedia Computer Science*, vol. 179, no. 1, pp. 321–329, 2021.

[3] A. Conforto, W. Bernardo, and T. Tokuno, "The effects of robotic therapy associated with non-invasive brain stimulation on upper limb rehabilitation after stroke: systematic review and meta-analysis of randomized clinical trials," *Neurorehabilitation and Neural Repair*, vol. 35, no. 3, pp. 256–266, 2021.

[4] D. Mu and C. Yue, "Machine recognition efficiency study of safety signs based on image degradation simulation," *Multimedia Tools and Applications*, vol. 81, no. 2, pp. 2127–2143, 2022.

[5] W. Chen, M. Yao, Z. Zhu, Y. Sun, and X. Han, "The application research of AI image recognition and processing technology in the early diagnosis of the COVID-19," *BMC Medical Imaging*, vol. 22, no. 1, pp. 29–10, 2022.

[6] J. Chen and X. Wang, "Non-intrusive load monitoring using gramian angular field color encoding in edge computing," *Chinese Journal of Electronics*, vol. 31, no. 4, pp. 595–603, 2022.

[7] X. Xu, H. Li, W. Xu, Z. Liu, L. Yao, and F. Dai, "Artificial intelligence for edge service optimization in internet of vehicles: a survey," *Tsinghua Science and Technology*, vol. 27, no. 2, pp. 270–287, 2022.

[8] T. Taleb, K. Samdanis, B. Mada, H. Flinck, S. Dutta, and D. Sabella, "On multi-access edge computing: a survey of the emerging 5G network edge cloud architecture and

orchestration," *IEEE Communications Surveys & Tutorials*, vol. 19, no. 3, pp. 1657–1681, 2017.

[9] T. Ogino, S. Kitagami, T. Suganuma, and N. Shiratori, "A multi-agent based flexible IoT edge computing architecture harmonizing its control with cloud computing," *International Journal of Networks and Communications*, vol. 8, no. 2, pp. 218–239, 2018.

[10] C. Esposito, A. Castiglione, F. Pop, and K. K. R. Choo, "Challenges of connecting edge and cloud computing: a security and forensic perspective," *IEEE Cloud Computing*, vol. 4, no. 2, pp. 13–17, 2017.

[11] S. Chaudhary and S. Murala, "Depth-based end-to-end deep network for human action recognition," *IET Computer Vision*, vol. 13, no. 1, pp. 15–22, 2019.

[12] S. M. Patel and J. N. Dharwa, "Medical image enhancement through deep learning methods," *National Journal of System and Information Technology*, vol. 11, no. 1, pp. 35–44, 2018.

[13] K. C. Rim, P. k. Kim, H. Ko, and K. Bae, "Restoration of dimensions for ancient drawing recognition," *Electronics*, vol. 10, no. 18, p. 2269, 2021.

[14] P. Lurz, R. Stephan von Bardeleben, M. Weber et al., "Transcatheter edge-to-edge repair for treatment of tricuspid regurgitation," *Journal of the American College of Cardiology*, vol. 77, no. 3, pp. 229–239, 2021.

[15] Y. Liu, Y. H. Hsu, A. P. H. Huang, and S. H. Hsu, "Semi-interpenetrating polymer network of hyaluronan and chitosan self-healing hydrogels for central nervous system repair," *ACS Applied Materials & Interfaces*, vol. 12, no. 36, Article ID 40120, 2020.

[16] L. Wang and A. Sharma, "Analysis of sports video using image recognition of sportsmen," *International Journal of System Assurance Engineering and Management*, vol. 13, no. S1, pp. 557–563, 2022.

[17] N. M. C. N. T. L. N. X. Thao, T. L. Nguyen, and X. T. Nguyen, "A new similarity measure of picture fuzzy sets and application in pattern recognition," *American Journal of Business and Operations Research*, vol. 1, no. 1, pp. 5–18, 2020.

[18] H. Liu, Y. Zhang, and T. Yang, "Blockchain-enabled security in electric vehicles cloud and edge computing," *IEEE Network*, vol. 32, no. 3, pp. 78–83, 2018.

[19] M. Ke, Z. Gao, Y. Wu, X. Gao, and K. K. Wong, "Massive access in cell-free massive MIMO-based internet of things: cloud computing and edge computing paradigms," *IEEE Journal on Selected Areas in Communications*, vol. 39, no. 3, pp. 756–772, 2021.

[20] X. Yang, Z. Fei, J. Zheng, N. Zhang, and A. Anpalagan, "Joint multi-user computation offloading and data caching for hybrid mobile cloud/edge computing," *IEEE Transactions on Vehicular Technology*, vol. 68, no. 11, Article ID 11030, 2019.

[21] N. Mir and S. Loreto, "Cloud and edge computing," *IEEE Communications Standards Magazine*, vol. 3, no. 2, 2019.

[22] B. Du, R. Huang, Z. Xie, J. Ma, and W. Lv, "KID model-driven things-edge-cloud computing paradigm for traffic data as a service," *IEEE Network*, vol. 32, no. 1, pp. 34–41, 2018.

[23] N. Mir and S. Loreto, "Cloud and edge computing," *IEEE Communications Standards Magazine*, vol. 1, no. 4, 2017.

[24] B. D. Deebak, F. Al-Turjman, and L. Mostarda, "Seamless secure anonymous authentication for cloud-based mobile edge computing," *Computers & Electrical Engineering*, vol. 87, no. 2, 1 page, Article ID 106782, 2020.

[25] R. V. Moreno, E. Huedo, R. S. Montero, I. M. Llorente, and G. Pallis, "A disaggregated cloud architecture for edge computing," *IEEE Internet Computing*, vol. 23, no. 3, pp. 31–36, 2019.

[26] X. Zhang, H. Chen, Y. Zhao et al., "Improving cloud gaming experience through mobile edge computing," *IEEE Wireless Communications*, vol. 26, no. 4, pp. 178–183, 2019.